Supplemental Material for:

Screen identifies bromodomain protein ZMYND8 in chromatin recognition of transcription-associated DNA damage that promotes homologous recombination

Fade Gong[1,2,6], Li-Ya Chiu[1,2,6], Ben Cox[1,2], François Aymard[3,4], Thomas Clouaire[3,4], Justin W. Leung[1,2], Michael Cammarata[5], Mercedes Perez[1,2], Poonam Agarwal[1,2], Jennifer S. Brodbelt[5], Gaëlle Legube[3,4] & Kyle. M. Miller[1,2,*]

Supplemental Materials and Methods

Plasmid and siRNA transfections

Mammalian expression vectors were transfected into U2OS cells by Hilymax (Dojindo) or Fugene HD (Promega) according to manufacturer's instructions. The I-SceI expressing vector (pCAG-I-SceI) or control vector (pCAG) were transfected into the U2OS DR-GFP cells by Fugene HD (Promega). For HEK293T cells, transient transfections were carried out with pEI (Polyethylenimine, Sigma). Analyses for transient plasmid transfection were performed 24-48 h after transfection. Transfections for siRNA were carried out with lipofectamine RNAiMax (Invitrogen) following the manufacturer's instructions. Analyses from siRNA treated cells were performed 48-72 h after transfection. The siRNAs used in this study were: siControl: non-targeting pool (Dharmacon); siZMYND8 #1: SMARTpool (Dharmacon); siZMYND8 #2: GGACUUUCCCCUUUUUAUA (targeting the 3'-UTR region of ZMYND8) (Sigma); siZMYND8 #3: GAACAUAGAUGAAUGAAA (Sigma); siCHD4: CCCAGAAGAGGAUUUGUCA (Sigma), siLSD1: GCCUAGACAUUAAACUGAAUA (Sigma); siTIP60 SMARTpool (Dharmacon); siMOF: GCAAAGACCAUAAGAUUUA (Sigma); siCtIP: GGUAAAACAGGAACGAAUC (Sigma); siLigaseIV: AGGAAGUAUUCUCAGGAAUUA (Sigma).

Cloning and plasmids

cDNAs of human BRD-containing proteins were cloned into the Gateway entry vector pENTR11 by restriction sites, or pDONR201 by attB recombinant sites. For creating ZMYND8 internal deletion constructs, two HindIII sites were introduced into the sites of the deletion segment using site-directed mutagenesis following standard protocols. Plasmids successfully inserted with two HindIII sites were digested and re-ligated to remove the intervening sequences. The cDNAs were sub-cloned from the entry vector into mammalian expression vectors containing GFP or SFB tags in the N-terminus or C-terminus. For creating ZMYND8 PHD-BRD fusion protein (GST-PB-His), 6X His-tag was extended at the C-terminus of the PHD-BRD fragment (residue 108-280) by PCR, and then the PB-His fragment was sub-cloned into DEST15 vector which contains GST in the N-terminus. All plasmids used in this study are listed in Supplemental Table S2.

EdU and Cell proliferation assay

The Click-iT EdU image kit (Invitrogen) was used to detect the incorporation of EdU (5-ethynyl-2'-deoxyuridine) into DNA during DNA synthesis for measuring replicating cells. Briefly, post-72 h after the indicated siRNA treatment, of EdU was added into the culture medium to a final concentration of 10 uM and incubated for 30 mins. Cells were then fixed and stained to detect EdU positive cells according to manufacturer's instructions. Samples were imaged and analyzed with Z-stacked settings using the FV10-ASW3.1 software on a Fluoview 1000 confocal microscope (Olympus).

Cell proliferation assays were carried out using the Cell Counting Kit-8 (Dojindo). Briefly, post-24 h after siRNA transfection, cells were trypsinized and seeded back to 96-well plates (1000 cells/well). For each siRNA sample, six repeats were prepared for each time point. For detecting the cell number, 10 ul of CCK-8 solution was added into each well. After 4 h incubation at 37°C, the absorbance at 450 nm was measured on a Tecan Infinite M1000 PRO plate reader. The absorbance measurements at 450 nm reflect cell density. For normalization, we first averaged the six repeats from each time point for each sample, and then normalized the values obtained at each time point to the first measured time point for each siRNA treatment.

Protein extracts and western blotting

For whole cell extracts, cells were collected with Laemmli buffer (4% (v/v) SDS, 20% (v/v) glycerol and 120 mM Tris-HCl, pH 6.8), and sonicated at 4°C in a Diagenode Bioruptor 300 (30 sec on/30 sec off) for 10 min followed by boiling for 5 min at 95°C before loading. For chromatin fractions, cells were pre-extracted by CSK buffer (10 mM PIPES, pH 6.8, 100 mM NaCl, 300 mM sucrose, 3 mM $MgCl_2$, 1 mM EGTA, 0.5% (v/v) Triton X-100) for 5 min on ice to remove soluble proteins. After two washes with PBS, chromatin extracts were collected with Laemmli buffer, and processed similarly as whole cell extracts before loading. Samples were resolved by SDS-PAGE and analyzed by standard WB. Primary antibodies used for this study are listed in Supplemental Table S3. Western blots were detected by standard chemiluminescence (GE Healthcare, Amersham ECL

Prime system) and analyzed using a Bio-Rad molecular imager ChemiDoc XRS+ system.

Live-cell microscopy analysis

For quantification of laser damage recruitment, after laser microirradiation, the fluorescence intensity at the damage site as well as an undamaged control region of the same size from the same cell were directly recorded by the FV10-ASW3.1 software in real-time. Variation of the fluorescence intensity was quantified as the difference between the average fluorescence intensity in the damaged region versus the average fluorescence intensity in an undamaged region of the same size from the same cell. Each curve corresponds to data obtained from at least 10 independently analyzed cells. Experiments were performed in a heated environmental chamber with 5% CO_2 on a Fluoview 1000 confocal microscope (Olympus).

Immunofluorescence (IF)

After indicated treatments, cells were treated and processed for IF as previously described (Leung et al. 2014). Briefly, cells were pre-extracted with CSK buffer for 5 min on ice. Cells were fixed with 2% (v/v) formalin for 15 min at room temperature and then blocked with PBS containing 3% BSA. For specific treatment without pre-extraction, cells were permeabilized with 0.5% (v/v) Triton-X for 10 min between fixing and blocking steps. After blocking, cells were incubated with indicated primary antibodies. Primary antibodies used for IF are

listed in Supplemental Table S3. Secondary antibodies used for IF were: Alexa Fluor 488 goat anti-rabbit IgG, Alexa Fluor 488 goat anti-mouse IgG, Alexa Fluor 594 goat anti-rabbit IgG, and Alexa Fluor 594 goat anti-mouse IgG. Cells were imaged and analyzed with Z-stacked settings using the FV10-ASW3.1 software on a Fluoview 1000 confocal microscope (Olympus).

Histone modification binding assay

N-terminal GST and C-terminal His-tagged ZMYND8 PHD-BRD recombinant protein (GST-PB-His) was induced in *E. coli* BL21 (DE3) at 16°C overnight with 0.25 mM IPTG. Recombinant proteins were initially purified on Ni-NTA resin (Qiagen), following glutathione sepharose 4B resin (GE Healthcare) according to manufacturer's instructions. The purity of recombinant protein was confirmed with coomassie blue staining. A modified histone peptide array (Active Motif) was blocked with 5% non-fat milk in TNT buffer (50 mM Tris-HCl, pH 7.5, 150 mM NaCl, 0.05% Tween-20) and then incubated with purified GST-PB-His at 4°C for 1 h. The array was washed with TNT buffer and probed with primary GST antibody (GE Healthcare) for 1 h. The array was washed 3X with TNT and incubated with HRP conjugated α-Goat antibody (Abcam) for 1 h. The array was detected by standard chemiluminescence as described for Western blotting.

For peptide pull down assays, preparation of cell extracts were performed as previously described (Bartke et al. 2010). HEK293T cells expressing WT, mutant GFP-ZMYND8 or GFP-ZMYND11 were collected and lysed in extraction buffer (20 mM HEPES, pH 7.5, 300 mM NaCl, 0.5% NP-40, 1 mM EDTA, 1 mM DTT

and 20% glycerol) at 4°C for 1 h. Cell lysates were diluted with equal volume of dilution buffer (20 mM HEPES, pH 7.5, 1 mM EDTA, and 20% glycerol) and the centrifugation cleared lysates were analyzed by pull-down assay. HeLa nuclear extracts were obtained from Accurate Chemical. The following biotin-conjugated H4 histone peptide corresponding to N-terminal H4 tail (1-25 amino acids) were purchased from AnaSpec: H4, H4K16Ac, H4 Tetra-Ac. Different histone peptides were immobilized on Dynabeads® MyOne™ Streptavidin T1 (Invitrogen). Peptide bound beads were incubated with indicated cell extracts in binding buffer (20 mM HEPES, pH 7.5, 150 mM NaCl, 0.25% NP-40, 1 mM EDTA, 1 mM DTT and 20% glycerol) at 4°C for 1 h. Bound proteins were washed 6X with the indicated buffer and eluted by boiling with Laemmli buffer. Proteins were separated by SDS-PAGE followed by WB with the indicated antibodies.

Tandem affinity purification (TAP)

Tandem affinity purification (TAP) was performed as previously described with minor modifications (Leung et al. 2012). Briefly, HEK293T cells were seeded in 10 cm dishes and transiently transfected with SFB (S-protein, 2XFlag, streptavidin-binding peptide) tagged constructs. After 24 h of transfection, 10 dishes of cells with transfection plus 10 dishes of cells without transfection were collected and combined together. Cells were lysed with NETN buffer (150 mM NaCl, 1mM EDTA, 10 mM Tris-HCl, pH 8.0, and 0.5% NP-40) for 30 min at 4°C. Cell lysates were cleared by 15000 rpm centrifugation for 30 min at 4°C. The supernatants were collected as the soluble fraction. The pellets were digested

with NETN buffer containing TurboNuclease (Accelagen) and 1 mM $MgCl_2$ for 1 h at 4°C. Cell lysates were then centrifuged to collect the supernatants as the chromatin fraction. Both soluble and chromatin fractions were incubated with 300 µl of streptavidin beads (GE Healthcare) for at least 1 h at 4°C. Next, the beads were precipitated by 2000 rpm centrifugation and washed once with NETN buffer. The bound proteins were eluted with 750 µl of NETN buffer containing 2 mg/ml biotin (Sigma) twice. The eluted supernatants were incubated overnight with 40 µl of S-protein beads (Novagen). The precipitated beads were washed three times with NETN buffer. Protein mixtures were eluted by boiling with Laemmli buffer, and resolved by SDS-PAGE. The purification efficiency was checked by silver stain (Calbiochem) following manufacturer's instruction. The remaining samples were subjected to Mass Spectrometry (MS).

Mass spectrometry (MS) analysis

For MS experiments, Samples for data from Mass Spect_1 and Mass Spect_4 were obtained from Taplin Mass Spectrometry Facility, Harvard. Samples of Mass Spect_2 and Mass Spect_3 were analyzed as follows with technical triplicates.

Samples were exposed to ice cold acetone for 24 hours to remove impurities and non-protein material from the sample. After exposure, the samples were spun down in a microcentrifuge and the supernatant was removed. The protein precipitate was then reconstituted in 8M urea with 150 mM ammonium bicarbonate at pH 8. Samples were then diluted to have urea concentration less

than 0.8 M to facilitate tryptic digestion. Prior to tryptic digestion the protein samples were reduced by addition of 20 mM dithiothreitol with heating at 37°C, then alkylated using 50 mM iodoacetimide for one hour in the dark at room temperature. Protein aliquots were digested using trypsin at a 1:25 protein:protease ratio for 14 hours at 37°C and quenched with formic acid to a final concentration of 0.2% formic acid. These digested samples were then stored in a -80°C freezer.

The digests were analyzed by LC-MS/MS performed on a Dionex Ultimate 3000 NSLC nano liquid chromatograph interfaced to a Thermo Scientific Velos Pro dual linear ion trap mass spectrometer. Approximately 3 µg of the complex protein digest was injected onto a New Objective IntegraFrit 100 µm inner diameter trap column (Woburn, MA) packed in-house with 5 µm Michrom Magic C18 AQ (Auburn, CA) to 3.5 cm. Preconcentration occurred for 10 minutes using 2% acetonitrile/0.1% formic acid at a flow rate of 5 µL/min. The preconcentration column was then switched in-line with a New Objective PicoFrit analytical column (Woburn, MA) (75 µm × 15 cm) packed in-house with 3.5 µm Waters Xbridge C18 (Millford, MA) resin. Separation was performed using a gradient consisting of mobile phase A (0.1% formic acid: 99.9% water) and mobile phase B (0.1% formic acid: 99.9% acetonitrile) applied as a 150 min linear gradient from 2% to 45% eluent B at a flow rate of 300 nL/min. The full MS range scanned was m/z 400-2000 using 1 µscan with the capillary temperature set at 250°C and spray voltage of 1.75kV. MS/MS analysis of eluting peptides was undertaken in a data dependent top ten manner using a normalized collision energy of 35% with a

default CID charge state of 5+, isolation window of 4 m/z, and a q value of 0.25 with 2 μscans averaged per spectrum. The control sample and the ΔPBP sample were each injected three times. Proteome Discoverer SEQUEST was used for proteomic analysis of the immunoprecipitated samples. The resulting LC-MS/MS runs were searched against the reviewed human database from Uniprot using the following settings. Oxidation of methionine on methionines, alkylation of cysteines, alkylation of the N-terminus, and diglycine of the lysines were set as variable modifications. The peptide mass tolerance was set to ±1.20 Da with a MS/MS tolerance of 0.8 Da. The peptide length was constrained to a minimum length of 5 amino acids and a maximum of 50. Up to three missed cleavages were allowed for trypsin. Peptides were filtered against a 1% FDR for positive identification and protein identifications were based on a single positive unique peptide identification. Uniprot accession numbers were then used for further analysis.

For MS data analysis in this study, only those proteins identified with at least two peptides for each experiment, were considered to draw the overlap diagrams. List of proteins that had at least two peptides identified from each experiment can be found in Table S1.

Immunoprecipitation (IP) analysis

Cells were collected and lysed with NETN buffer containing 1 mM $MgCl_2$ and TurboNuclease for 1 h at 4°C. Cell lysates were cleared by 15,000 rpm centrifugation for 30 min at 4°C. Overexpressed SFB tagged protein were

immunoprecipitated with 30 µl of streptavidin beads (GE Healthcare) after rolling at least 1 h at 4°C. Endogenous proteins were immunoprecipitated by 1 µg of indicated antibodies and 25 µl of IgG and IgA Dynabeads (Invitrogen) after rotating at 4°C overnight. Beads were washed 4X with NETN buffer. Protein mixtures were eluted by boiling with Laemmli buffer and followed by standard WB analysis with indicated antibodies.

Clonogenic cell survival assays

72 h after indicated siRNA transfection, U2OS cells were treated with different dosages of IR. Cells were left to form colonies for 10 to 14 days at 37°C. Colonies were washes with PBS and stained with 0.5% (w/v) crystal violet and 20% (v/v) ethanol for 30 min at room temperature. After staining, plates were gently washed with water, and colonies were counted. Results were normalized to plating efficiencies of untreated cells for each siRNA.

Homologous recombination assay

An integrated HR reporter DR-GFP-containing U2OS cell line was used as described previously (Pierce et al. 1999). One day after indicated siRNA treatments, U2OS DR-GFP cells were transfected with I-SceI expressing vector (pCAG-I-SceI) or control vector (pCAG). 48 h following I-SceI transfection, cells were trypsinized, washed once with PBS, and then resuspended in sodium citrate solution without fixation. Resuspended cells were filled into a 5 ml polystyrene Falcon round-bottom tubes through the cell-strainer caps. The

percentage of GFP positive cells was determined by a BD Accuri Flow Cytometer (BD biosciences). All samples were normalized with the siControl sample transfected with pCAG-I-SceI vector.

NHEJ Assays

Experiments were performed as previously described (Miller et al. 2010). Briefly, 24 h after siRNA transfection, U2OS cells were transfected with linearized pEGFP-C1 (BamHI and XhoI treatment). The next day, GFP positive cells were counted to calculate transfection efficiency. The cells were then trypsinized, counted and plated into two duplicate sets of plates. One plate contained 0.5 µg/ml G418 (to detect NHEJ events), and the other with no selection (to obtain plating efficiency) were allowed to grow for two weeks until colonies were formed. Colonies were stained as in the clonogenic cell survival assay methods. Random-plasmid NHEJ-dependent integration events were calculated using transfection and plating efficiency normalized to siControl.

Reverse transcription and Quantitative PCR

Total RNA for each sample was purified using the RNeasy mini kit (Qiagen) and treated with RNase-Free DNase I (Qiagen) following the manufacturer's protocol. 1 µg of total RNA for each sample was used to synthesize cDNA by the superscript III first strand synthesis system (Invitrogen). Quantitative PCR (qPCR) was performed on the StepOnePlus Real-Time PCR system (Applied Biosystems) using SYBR green master mix (Applied Biosystems) with the

indicated primers. The primer pair for GAPDH was described previously (Carvajal et al. 2012). The primer pair for the transgene integrated in the U2OS-DSB reporter cell line was used as previously described (Shanbhag et al. 2010). The sequences of qPCR primers are: ZMYND8 Forward, GGTGGTAGAGGGCATGGATA; ZMYND8 Reverse, CCATTGGAAGAATGTGGAGG; TIP60 Forward, TCAAGCCGTGGTACTTCTCC; TIP60 Reverse, ATCTCATTGCCTGGAGGATG; MOF Forward, CTGCTGAAGTGATCCAGTCTCG; MOF Reverse, CGGTTCTTGTCTACCCACTCGT. E2F target genes (Bracken et al. 2004) were analyzed with the following primers; CHEK1, QuantiTect Primer Assay QT00006734 (Qiagen); PRKDC, QuantiTect Primer Assay QT01849057 (Qiagen); RPA1, QuantiTect Primer Assay QT00067676 (Qiagen); MSH2, QuantiTect Primer Assay QT00032466 (Qiagen).

Chromatin Immunoprecipitation

ChIP assays were performed as previously described (Aymard et al. 2014). Primers used to measure XRCC4 enrichment were located at around 80bp from the DSB sites, while those used to access RAD51 recruitment were located at around 800bp. Sequences of primers are listed as follows: DSB-I_80bp, Forward GTCCCTCGAAGGGAGCAC, reverse CCGACTTTGCTGTGTGACC; DSB-I_800bp, Forward TATGGGACCAAGCGAGTAGG, Reverse GCCTCACACACACACCCATA; DSB-III_80bp, Forward CCGTCCGTTACGTAGAATGC, reverse GGGCGGGGATTATGTAATTT; DSB-

III_800bp, Forward GGGACAGCGCGTACTTTG, Reverse, TCGCTAGGCCCAGCAGTT; DSB-1_80bp, Forward TCCCCTGTTTCTCAGCACTT, reverse CTTCTGCTGTTCTGCGTCCT; DSB-1_800bp, Forward GGAGAAGTGGCAGGACAATG, Reverse CAAGGCAAATTTGGGGACTA; DSB-2_80bp, Forward ATCGGGCCAATCTCAGAGG, reverse GCGACGCTAACGTTAAAGCA; DSB-2_800bp, Forward TTTTTGGGGGAAAGAGGTG, Reverse TTTTTGGGGGAAAGAGGTG.

FACS Analysis

U2OS cells were transfected with the indicated siRNA. 72 h post-transfection, cells were harvested and fixed with 80% ethanol overnight. The fixed samples were washed 3X with PBS and stained with propidium iodide (PI) and analyzed using a BD Accuri C6 flow cytometer (BD biosciences) to determine cell cycle distributions of the samples.

Supplemental References

Aymard F, Bugler B, Schmidt CK, Guillou E, Caron P, Briois S, Iacovoni JS, Daburon V, Miller KM, Jackson SP et al. 2014. Transcriptionally active chromatin recruits homologous recombination at DNA double-strand breaks. *Nature structural & molecular biology* **21**: 366-374.

Bartke T, Vermeulen M, Xhemalce B, Robson SC, Mann M, Kouzarides T. 2010. Nucleosome-interacting proteins regulated by DNA and histone methylation. *Cell* **143**: 470-484.

Bracken AP, Ciro M, Cocito A, Helin K. 2004. E2F target genes: unraveling the biology. *Trends in biochemical sciences* **29**: 409-417.

Carvajal LA, Hamard PJ, Tonnessen C, Manfredi JJ. 2012. E2F7, a novel target, is up-regulated by p53 and mediates DNA damage-dependent transcriptional repression. *Genes & development* **26**: 1533-1545.

Leung JW, Agarwal P, Canny MD, Gong F, Robison AD, Finkelstein IJ, Durocher D, Miller KM. 2014. Nucleosome Acidic Patch Promotes RNF168- and RING1B/BMI1-Dependent H2AX and H2A Ubiquitination and DNA Damage Signaling. *PLoS genetics* **10**: e1004178.

Leung JW, Wang Y, Fong KW, Huen MS, Li L, Chen J. 2012. Fanconi anemia (FA) binding protein FAAP20 stabilizes FA complementation group A (FANCA) and participates in interstrand cross-link repair. *Proceedings of the National Academy of Sciences of the United States of America* **109**: 4491-4496.

Miller KM, Tjeertes JV, Coates J, Legube G, Polo SE, Britton S, Jackson SP. 2010. Human HDAC1 and HDAC2 function in the DNA-damage response to promote DNA nonhomologous end-joining. *Nature structural & molecular biology* **17**: 1144-1151.

Pierce AJ, Johnson RD, Thompson LH, Jasin M. 1999. XRCC3 promotes homology-directed repair of DNA damage in mammalian cells. *Genes & development* **13**: 2633-2638.

Shanbhag NM, Rafalska-Metcalf IU, Balane-Bolivar C, Janicki SM, Greenberg RA. 2010. ATM-dependent chromatin changes silence transcription in cis to DNA double-strand breaks. *Cell* **141**: 970-981.

Supplemental Table Legends

Supplemental Table S1. ZMYND8 interactors identified by Mass Spectrometry. Data including genes identified and number of peptides from each individual mass spectrometry experiment are provided. These experiments include 3 ZMYND8 FL, 2 ZMYND8 delPBP and 1 ZMYND8 FL +IR IP mass spectrometry data sets. See experimental procedures for details.

Supplemental Table S2. Human BRD protein expression vectors used in this study. Information for each gene is provided and includes expression plasmid, vector and gene source.

Supplemental Table S3. List of antibodies used in this study.

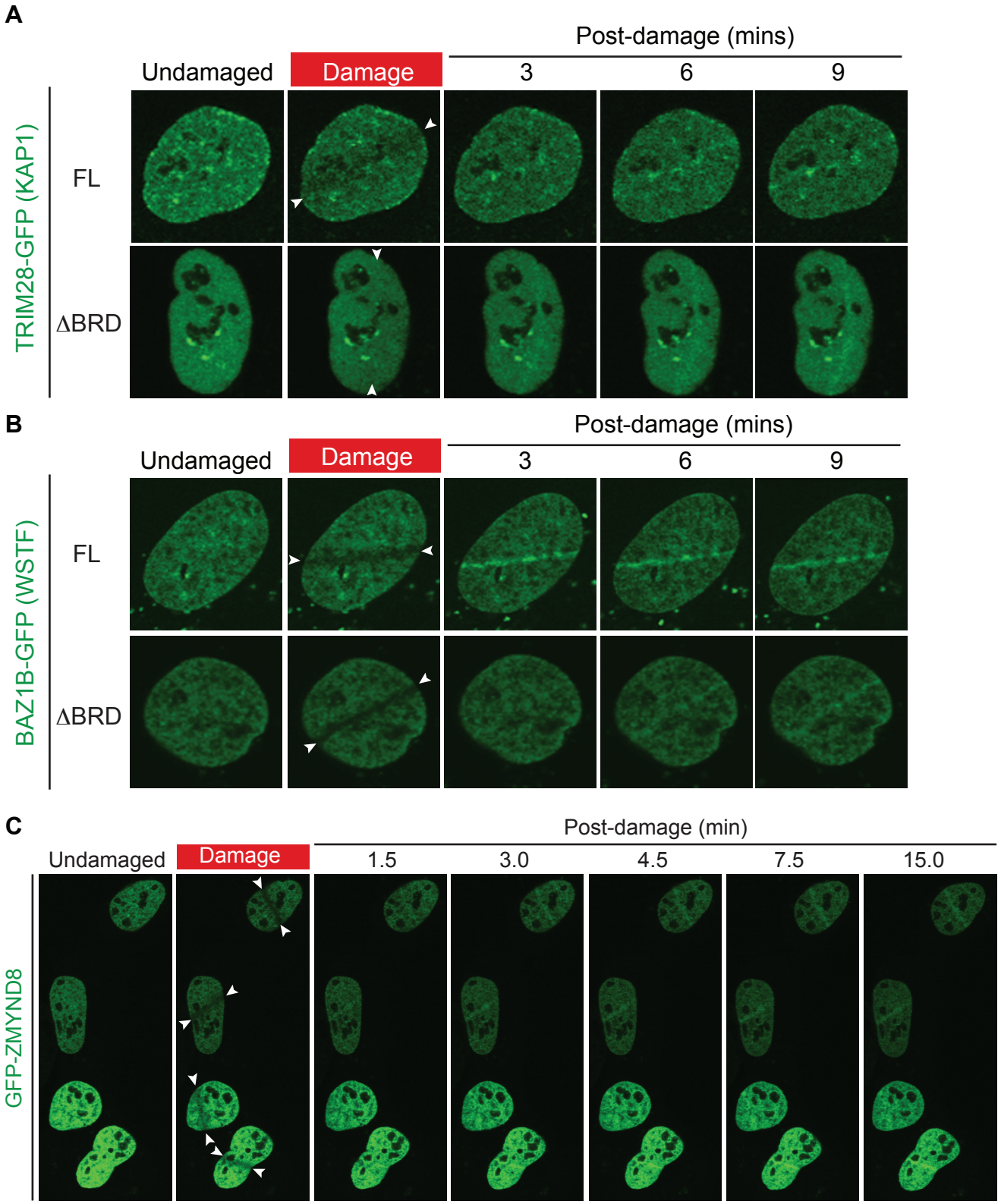

Supplemental Figure S1. Recruitment of TRIM28 or BAZ1B to laser damage sites does not require its BRD. (*A*,*B*) BRD-deleted (ΔBRD) TRIM28 and BAZ1B localize to laser damage. Experiments performed as in Fig. 2B. (*C*) Live cell imaging captured dynamic ZMYND8 mobilization after DNA damage. Arrowheads indicate the tracks of laser-damage.

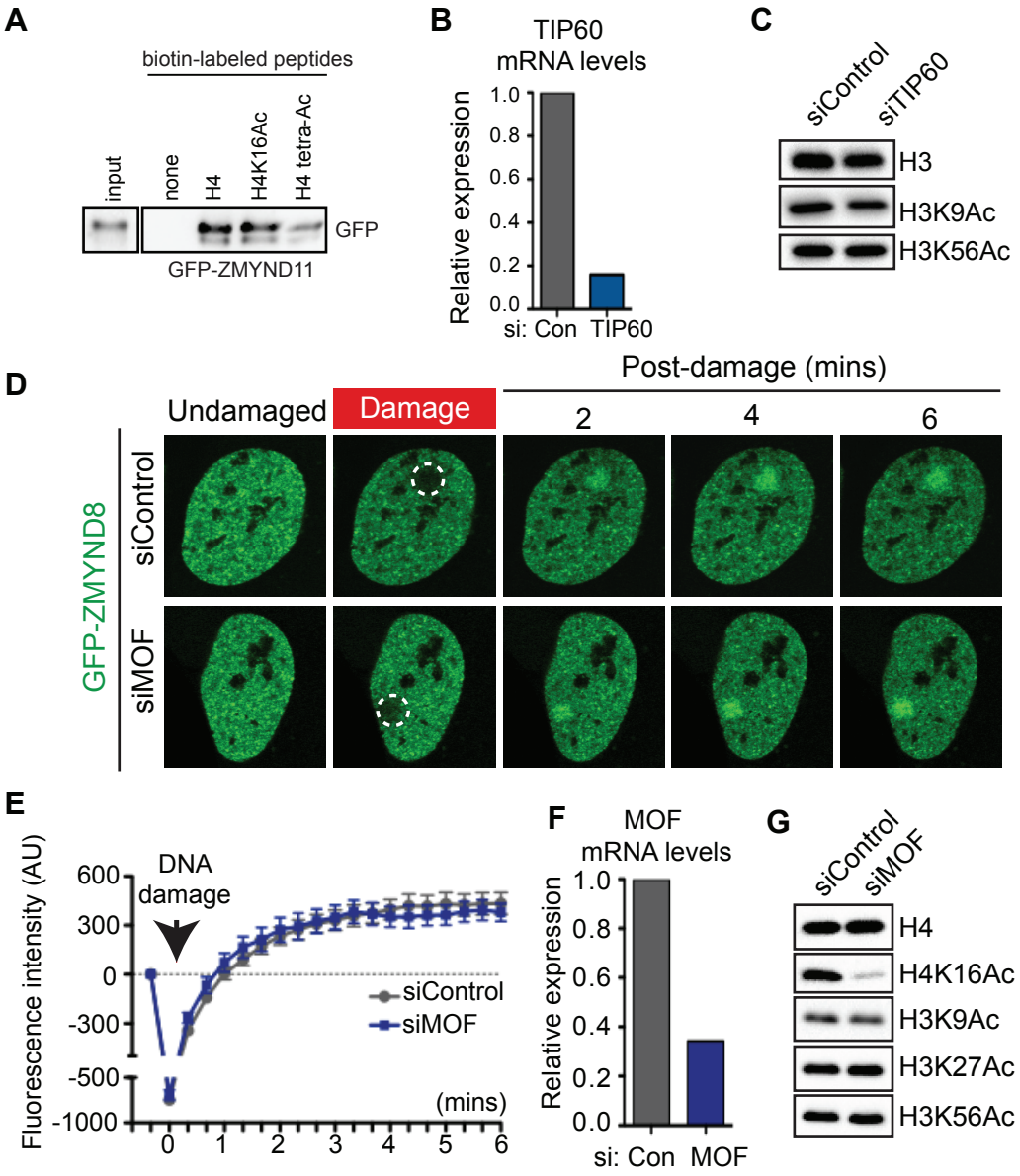

Supplemental Figure S2. TIP60 is required for ZMYND8 recruitment to DNA damage. (*A*) GFP-ZMYND11 does not bind acetylated H4. Experiments performed as in Figure 2I using HEK293T cell extracts expressing GFP-ZMYND11. (*B*) qPCR analysis of TIP60 expression from samples in Figure 2J. (*C*) TIP60 knockdown does not affect H3 acetylations. Samples from siControl and siTIP60 cells were analyzed by WB with the indicated antibodies. (*D*) MOF does not affect the recriutment of ZMYND8 to damaged chromatin. Experiments performed as in Figure 2J. (*E*) Quantification of D (Error bars, S.E.M., n>10). (*F*) MOF expression is reduced by siRNA treatment. Samples from D were analyzed as in B. (*G*) MOF depletion reduces H4Ac, but not H3Ac, as analyzed by WB.

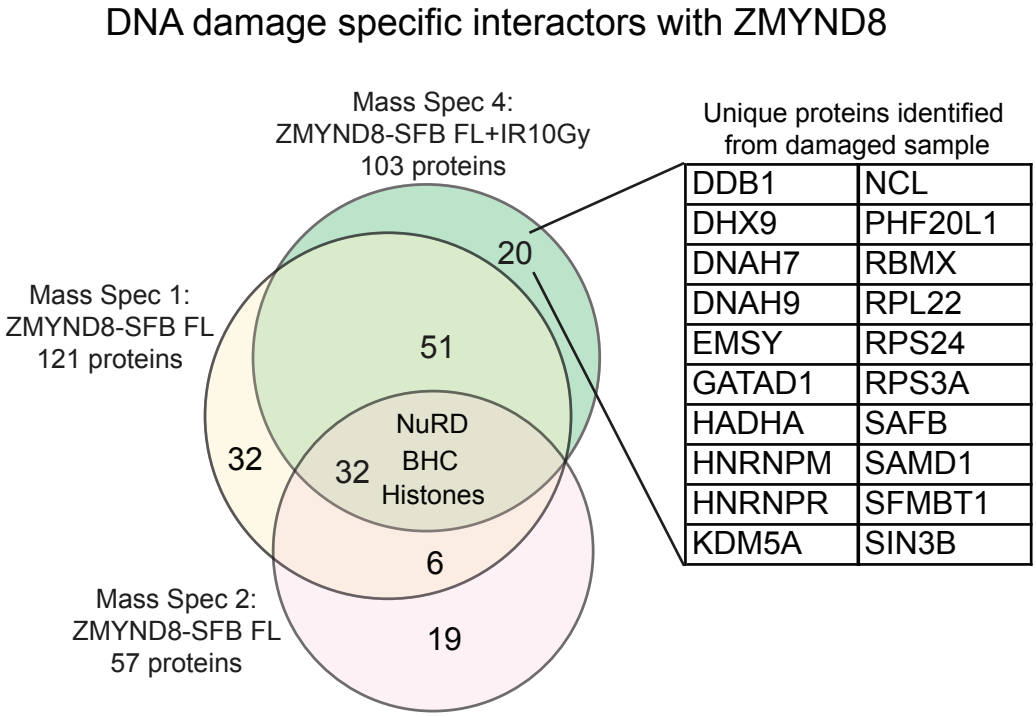

Supplemental Figure S3. Comparison of ZMYND8 Mass Spectrometry data between control and IR damaged samples. Overlap of ZMYND8 interactors from two biological replicate control samples (Mass Spect_1 and Mass Spect_2 as in Fig. 3C) and one IR treated sample (Mass Spect_4). The DNA damage unique ZMYND8 interacting proteins identified from this study are listed.

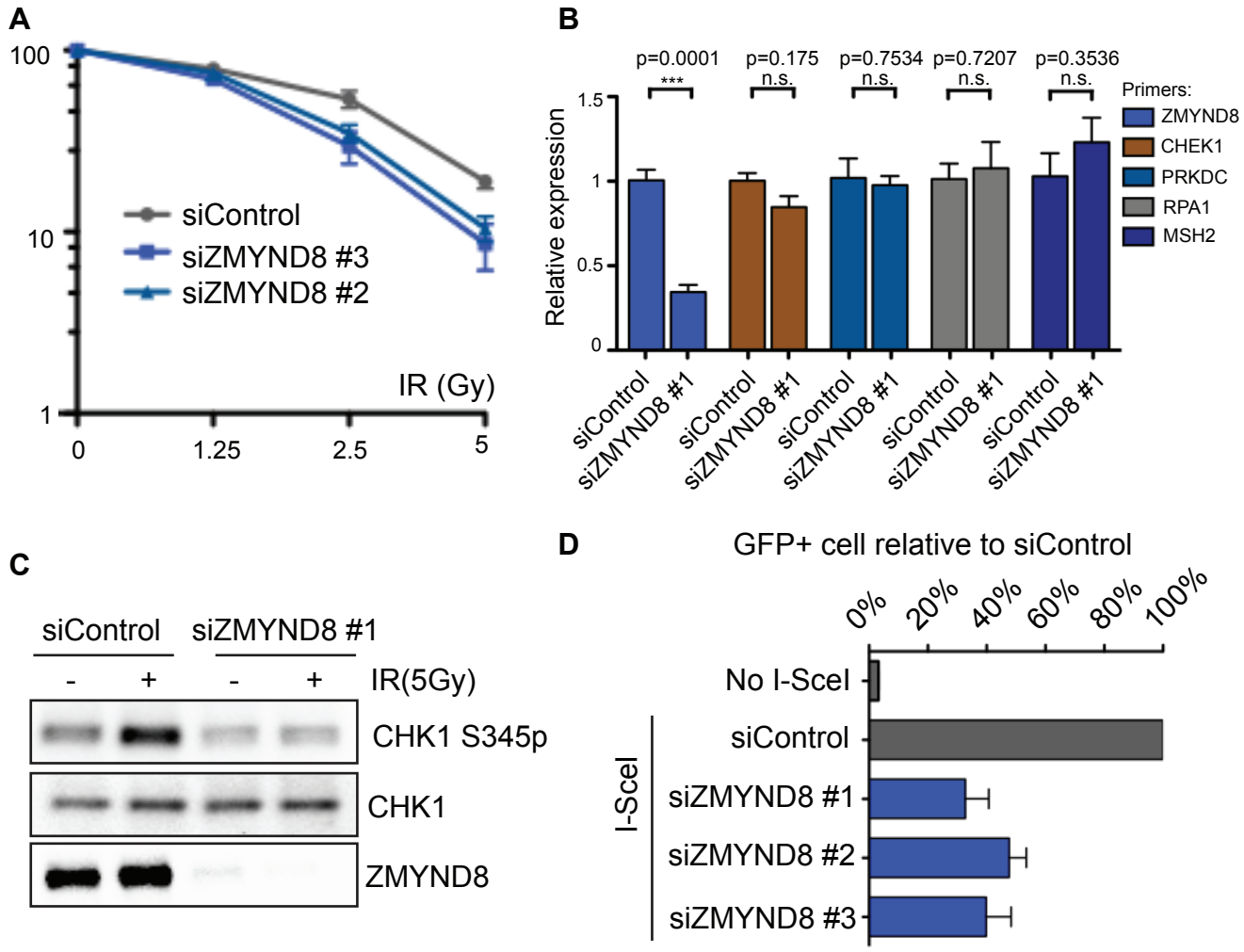

Supplemental Figure S4. Analysis of ZMYND8 in the DDR. (*A*) Clonogenic IR survival assays were performed as in Fig. 4B using different siRNA targeting ZMYND8 (Graphs are mean ± S.E.M., n=2). (*B*) Transcription levels of chosen E2F target genes (Bracken et al. 2004) upon ZMYND8 depletion were checked by qPCR (Error bars are S.E.M., n=4). (***) P < 0.001, n.s. = not significant, derived by Student's t-test. (*C*) siControl and siZMYND8 U2OS cells were IR-treated and analyzed by western blotting with indicated antibodies. Total CHK1 levels were normalized to load equal amount for both siControl and siZMYND8 samples. (*D*) DR-GFP reporter assays were performed as in Fig. 4D using different ZMYND8 siRNAs (Error bars are S.E.M., n=3). siZMYND8 #1 was used as positive control and collected from independent experiments compared to the one in Fig. 4D.

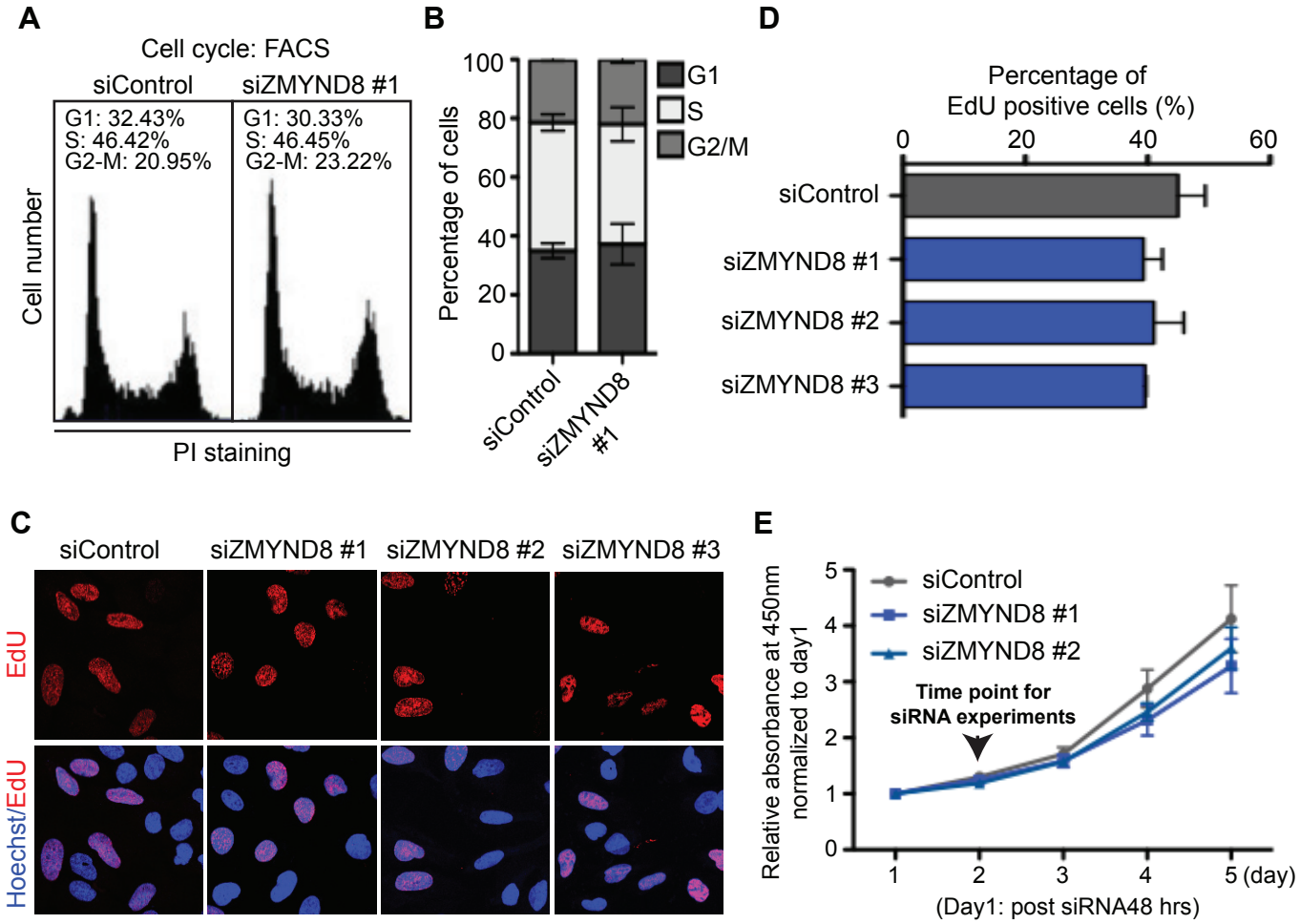

Supplemental Figure S5. Depletion of ZMYND8 does not appreciably affect the cell cycle. (*A*) FACS profiles of U2OS cells from siControl or siZMYND8. (*B*) Cell-cycle distribution of A was shown from two independent experiments. (*C*) EdU Incoporation assays were used to monitor cell proliferation rates upon different siRNA targeting ZMYND8. EdU positive cells indicate cells proliferating through S phase after EdU addition. (*D*) Quantification of C. For each siRNA sample, at least 200 cells were counted for each experiment (error bars are S.E.M. n=2). (*E*) Cell proliferation assay was performed in U2OS transfected with indicated siRNA. (Error bars are S.E.M. n=4).

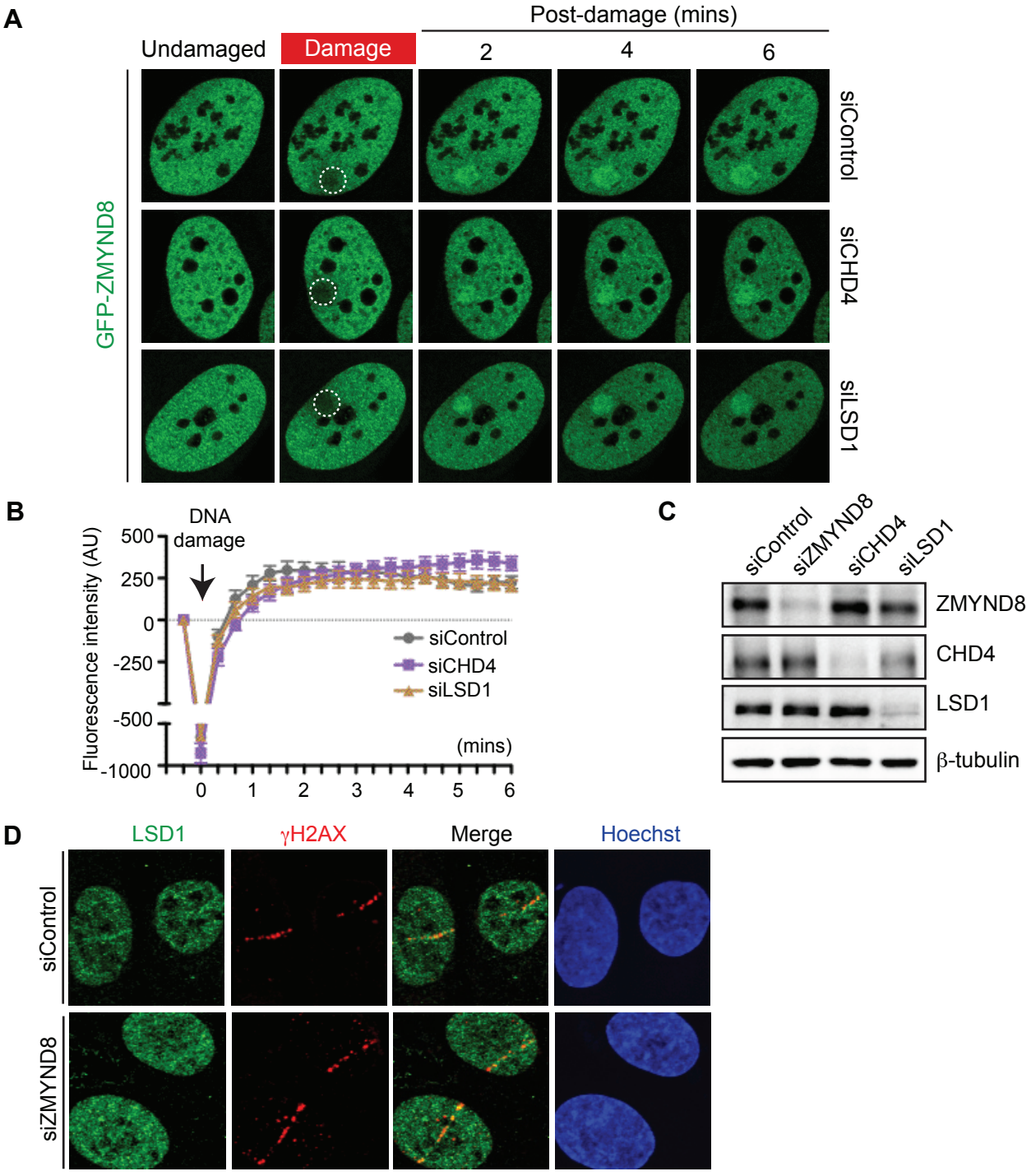

Supplemental Figure S6. ZMYND8 recruitment to DNA damage occurs independently from CHD4 or LSD1. (*A*) GFP-ZMYND8 recruitment to laser damage is unaffected by CHD4 or LSD1 knockdown using siRNAs. Experiments performed as in Fig. 2J with the indicated siRNAs. (*B*) Quantification of *A*. (Error bars, S.E.M., n>10). (*C*) siRNA knockdown efficiencies. WB analysis of samples from *A* with the indicated antibodies. (*D*) Recruitment of LSD1 to laser damage is independent of ZMYND8. Experiments performed as in Fig. 4E with the indicated siRNAs. Endogenous LSD1 accumulation at laser damage was analyzed by IF.

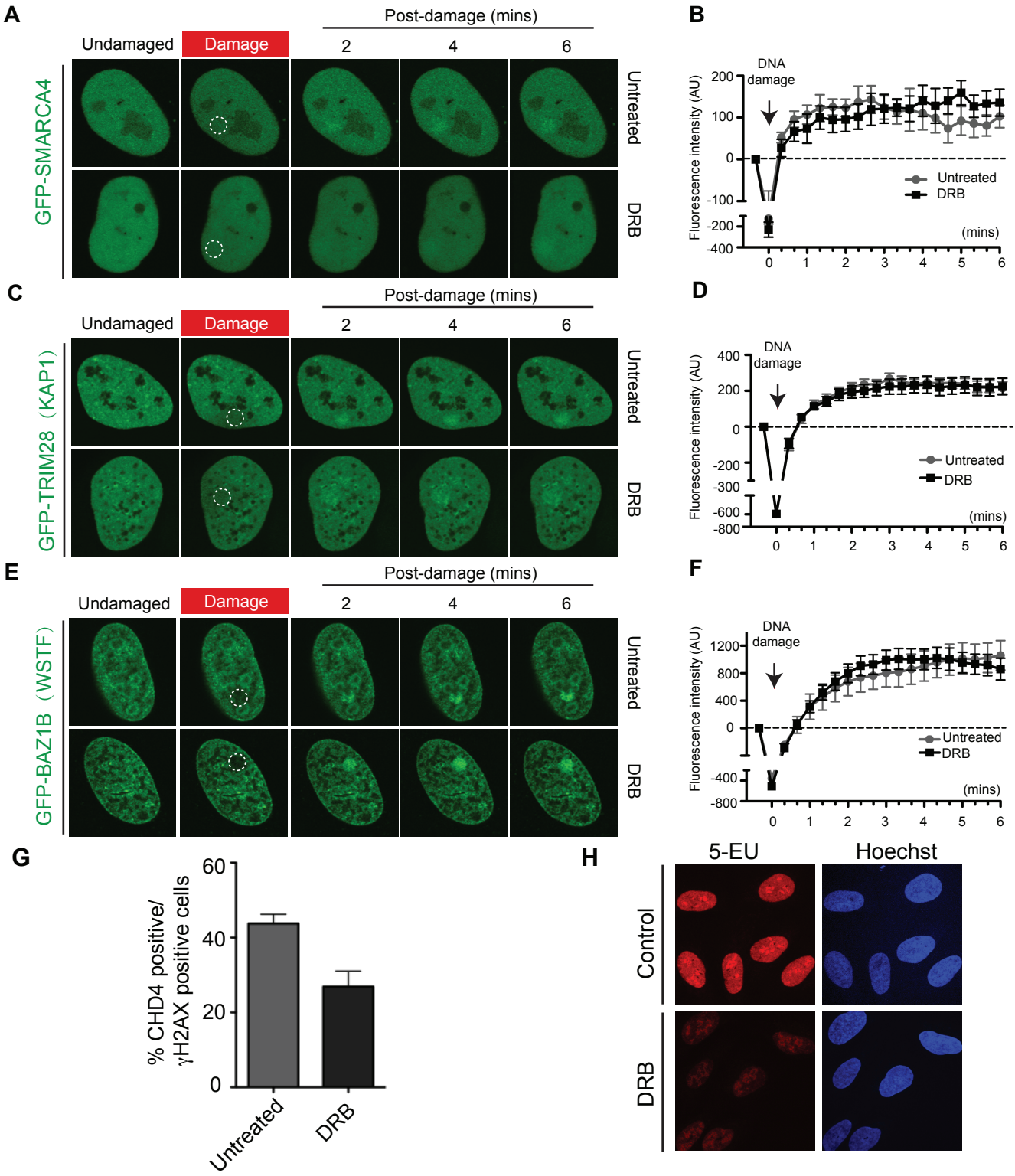

Supplemental Figure S7. Effects of transcription inhibition on BRD protein recruitment to DNA damage. (*A,C,E*) BRD protein accumulation on damaged chromatin are not blocked by transcriptional inhibition by DRB. (*A*) SMARCA4; (*C*) TRIM28; (*E*) BAZ1B. Cells stably expressing the indicated GFP-tagged proteins were treated and analyzed as in Fig. 5A. (*B,D,F*) Quantification of *A,C,E*. (Error bars, S.E.M., n>5). (*G*) Quantification of Fig. 5C. (Error bars, S.E.M., N=2). (*H*) Inhibition of 5-EU incorporation validates DRB efficacy.

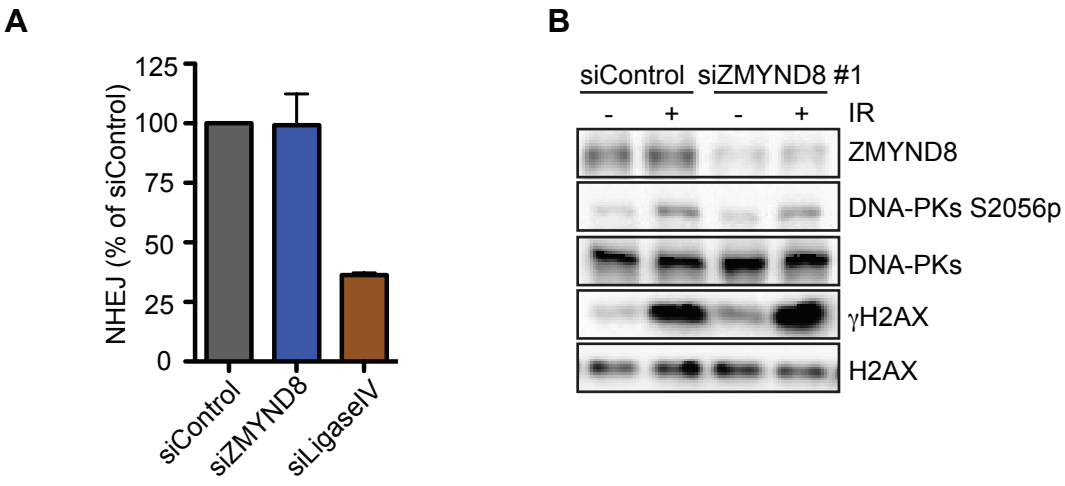

Supplemental Figure S8. ZMYND8 depletion does not affect NHEJ. (*A*) NHEJ repair was assayed by random plasmid integration in U2OS cells. Cells were treated with the indicated siRNAs and analyzed for NHEJ repair. Data were normalized to siControl cells and depletion of the NHEJ factor LigaseIV was used as a positive control for defective NHEJ (Error bars, S.E.M., n=2). (*B*) DNA-PKcs autophosphorylation, a signaling readout for NHEJ, is not affected upon DNA damage in cells depleted of ZMYND8. siControl and siZMYND8 U2OS cells were either untreated or treated with IR and analyzed by western blotting with the indicated antibodies.

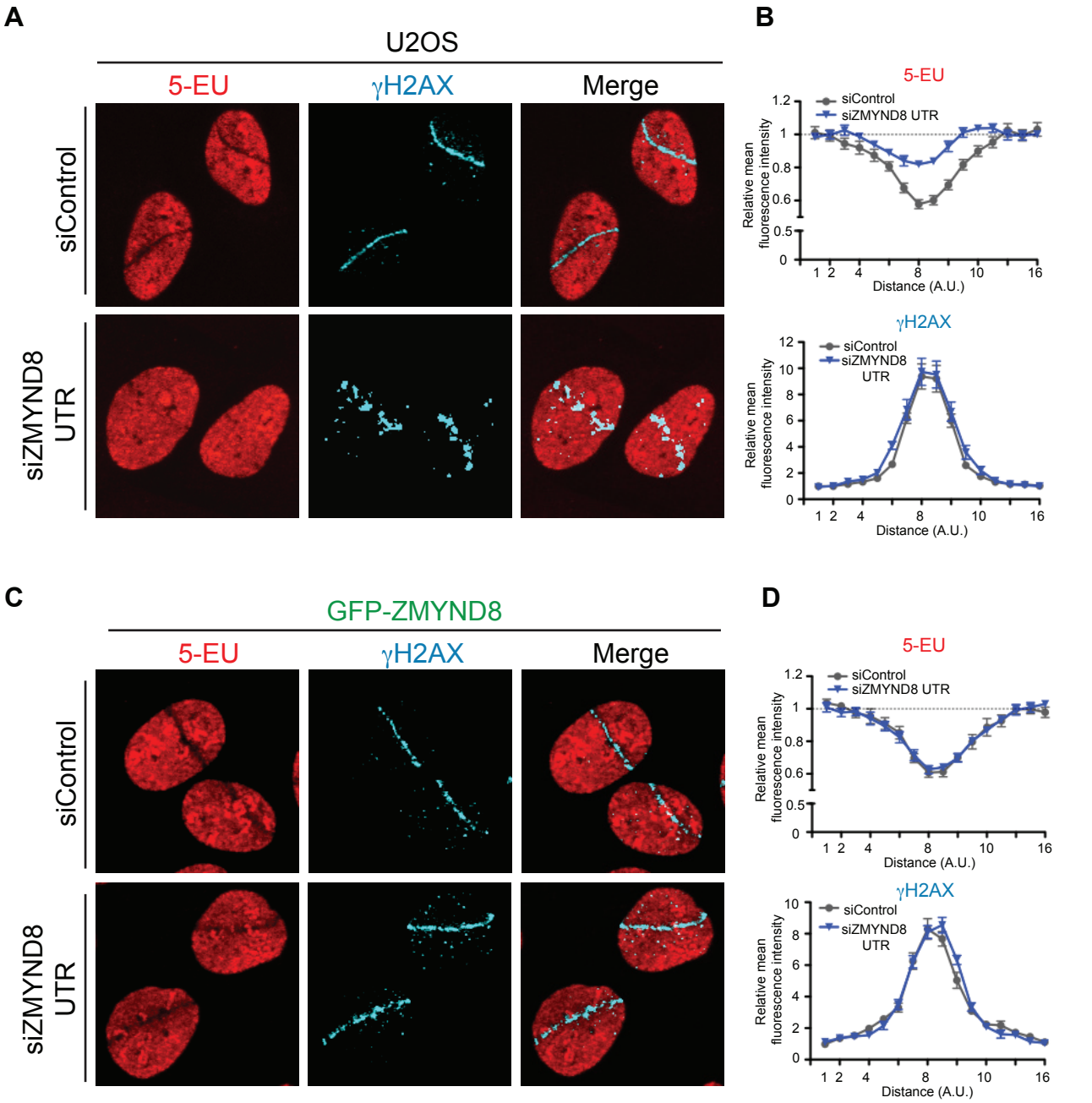

Supplemental Figure S9. Validation of siRNA ZMYND8 transcription-associated DNA damage defects by GFP-ZMYND8 rescue. (*A*) U2OS cells depleted of ZMYND8 by a siRNA targeting the 3'UTR region were defective in transcription repression upon DNA damage. Experiments were performed as in Fig. 6B. (*B*) Quantification of *A* as in Fig. 6C. (*C*) Ectopically expressed GFP-ZMYND8 restores transcriptional repression upon DNA damage. Experiments were performed as in A using U2OS cells stably expressing GFP-ZMYND8. (*D*) Quantification of *C* as in *B*.

Gong_Supplemental Figure S10

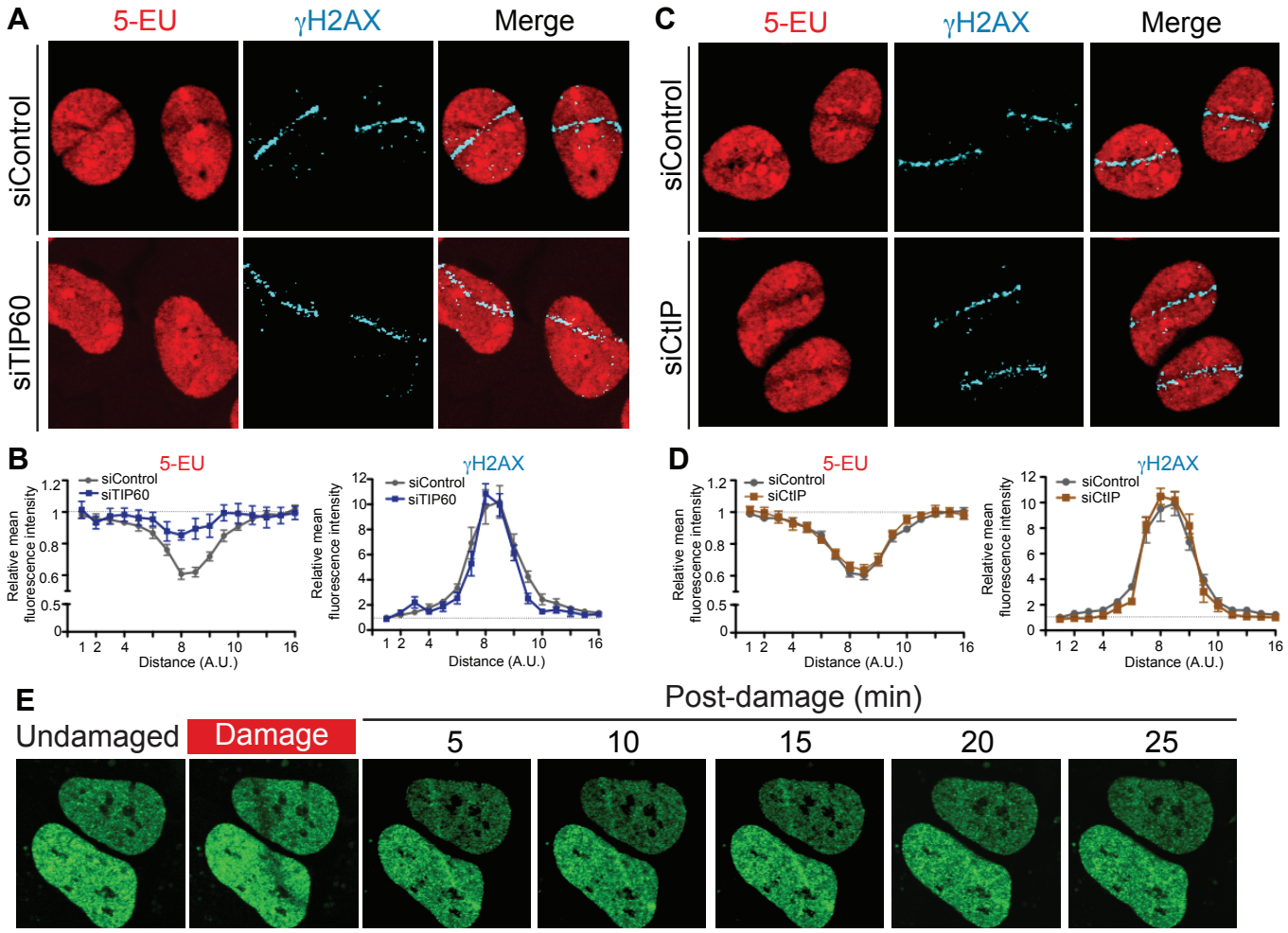

Supplemental Figure S10. Transcriptional repression analysis and GFP-ZMYND8 recruitment dynamics to laser damage. (*A-D*) Transcriptional repression following DNA damage was analyzed in U2OS cells depleted of TIP60 (*A,* quantified in B) or CtIP (*C,* quantified in D). Experiments performed as in Fig. 6B. (*E*) GFP-ZMYND8 is transiently recruited to DNA damage. Experiments were performed as in Fig. 2B using U2OS cells stably expressing GFP-ZMYND8 .

Supplementary Table 1: ZMYND8 interactors identified by Mass Spectrometry. Data including gene identified and number of peptides from each individual mass spectrometry experiment are provided. These experiments include 3 ZMYND8 full-length (FL), 2 ZMYND8 delPBP and 1 ZMYND8 FL +IR IP mass spectrometry data sets. See experimental procedures for details.

Mass Spec_ 1: ZMYND8-SFB FL

Gene symbol	# peptides
ZMYND8	144
CHD4	92
GATAD2A	41
MTA2	41
PRKDC	29
HSPA8	28
KDM1A	28
HDAC1	27
MTA1	27
ASUN	27
PARP1	23
CMAS	23
HSPA5	22
RREB1	22
CHD3	19
HSPA1A	18
INTS10	18
HIST1H4A	17
MBD3	17
HDAC2	16
HSPA1L	14
RBBP4	14
ZNF687	14
VWA9	13
MTA3	12
HSPA9	12
RCOR1	11
JMJD1C	10
KPNA3	9
KPNA2	9
PHF21A	9
RBBP7	8
HMG20B	8
SMARCA5	8
HSPD1	7
SFPQ	7
RCOR3	7
HIST1H2BB	6
HSPA2	6

KPNA4	6
MBD2	6
NPM1	6
ACTB	6
VIM	6
TFAM	6
PPP1R10	6
SMARCC1	6
RSF1	6
HIST1H2BA	5
HNRNPH1	5
USP7	5
TUBB2A	5
WDR82	5
H2AFY	5
XRCC5	5
RPS2	5
HNRNPK	5
RCC1	5
MGA	5
TPX2	5
NONO	5
SMARCA2	5
UBA52	4
TUBA1A	4
HIST3H3	4
C7orf26	4
ACTL6A	4
RCC2	4
PARP2	4
RUVBL2	4
ACTA2	4
HIST1H2AA	3
RPS8	3
RPL18	3
TMPO	3
XRCC6	3
ZNF592	3
HSPH1	3
BAZ1A	3
RCOR2	3
TOX4	3
CHD7	3
PRDX1	3
RPS7	3
PPP2R2A	3
SYNCRIP	3
RUVBL1	3
SRBD1	3

RBPJ	3
SMARCA4	3
INTS1	3
KIF22	3
SMARCA1	3
CBX8	3
RNF2	3
RING1	3
RPL7A	2
EEF1A1	2
HIST1H2BC	2
HIST1H1C	2
HIST1H2AD	2
RPL11	2
HNRNPU	2
CBX3	2
RPS3	2
EMD	2
H2AFY2	2
TOX2	2
CHD5	2
MECP2	2
HNRNPC	2
HNRNPCL1	2
H2AFV	2
WDR5	2
L3MBTL3	2
MPG	2
LRRC47	2
RPL4	2
CCNB1	2
RPS18	2
COL7A1	2
BAHCC1	2
PCGF6	2

Mass Spec_2: ZMYND8-SFB FL_1

Gene symbol	# peptides
ZMYND8	67
CHD4	54
GATAD2A	27
KRT1	24
MTA2	24
KRT10	16
RBBP4	15
MTA1	15
HSPA1A	14
KRT5	13
HSPA8	13

CHD5	13
RBBP7	10
HDAC1	10
MBD3	9
HSPA1L	9
KDM1A	9
KRT6A	8
HDAC2	7
MTA3	7
KRT14	6
KRT9	6
KRT16	6
HIST1H4A	5
ASUN	5
HIST1H2AH	4
NPM?	4
CMAS	4
VWA9	4
KRT2	4
H2AFZ	3
HIST1H3A	3
HIST1H2BJ	3
HIST1H2BK	3
HSPA5	3
UBC	3
RREB1	3
CDK2AP1	2
ACTB	2
HNRNPK	2
VIM	2
NONO	2
KPNA4	2
SMARCA2	2

Mass Spec_2: ZMYND8-SFB FL_2

Gene symbol	# peptides
ZMYND8	64
CHD4	61
GATAD2A	24
MTA2	23
HSPA8	18
HSPA1A	16
RBBP4	12
MTA1	12
RBBP7	11
CHD3	11
HDAC2	10
MBD3	9
KRT10	9

HDAC1	8
MTA3	8
VIM	7
NEUA	6
KRT1	6
KDM1A	6
ASUN	6
HIST1H4A	5
HIST1H2BK	5
HIST1H2BC	5
HIST1H2BD	5
HIST1H2BN	5
HIST1H2BH	5
HIST1H2BL	5
HIST1H2BM	5
HIST2H2BF	5
H2BFS	5
KRT9	5
H2AFZ	4
H2AFV	4
HIST2H2BE	4
HIST1H2BB	4
HIST1H2BJ	4
HIST1H2BO	4
HNRNPK	4
UBC	3
UBB	3
HIST1H3A	3
HIST1H2AH	3
HIST1H2AJ	3
HIST2H2AC	3
H2AFJ	3
HIST1H2AG	3
HIST3H2A	3
HIST2H2AA3	3
HIST1H2AB	3
HIST1H2AD	3
HIST1H2AC	3
UBA52	3
HIST3H2BB	3
RPS27A	3
NPM	3
PRSS3	3
KPNA3	3
KPNA4	3
KRT2	3
PARP1	3
CDK2AP1	2
H3F3C	2

HIST2H3A	2
H3F3A	2
HIST3H3	2
VWA9	2
RCOR3	2
HSPA9	2
ALB	2
RREB1	2
TNKS	2

Mass Spec_3: ZMYND8-SFB delPBP-1

Gene symbol	# peptides
ZMYND8	70
HSP7C	32
K2C1	31
HSP71	26
K1C10	19
GRP78	17
CHD4	16
ASUN	15
K2C5	13
GRP75	13
HSP72	12
GATAD2A	12
KRT9	11
HS71L	10
K2C6A	10
RBBP4	10
IMA4	10
KRT2	10
KRT14	9
VWA9	8
RBBP7	7
KPNA4	7
KRT16	7
MTA2	6
NEURL4	6
TUBA1B	5
KRT17	5
HDAC1	5
HERC2	5
MBD3	4
HDAC2	4
HSPD1	4
KDM1A	4
PPP2R2A	3
VIM	3
UBC	3
ZNF687	3

RPS28	2
ACTB	2
PRDX1	2
VAPB	2
VAPA	2
SLC25A5	2
MTA3	2
MTA1	2
HSPA4	2
HSPH1	2
GSE1	2

Mass Spec_3: ZMYND8-SFB delPBP-2

Gene symbol	# peptides
ZMYND8	61
HSPA8	29
HSPA1A	26
CHD4	15
HSPA5	13
KPNA3	11
HSPA9	10
KRT1	10
ASUN	10
RBBP4	9
KRT10	9
GATAD2A	8
RBBP7	7
HSPA6	7
HERC2	7
KPNA4	6
VIM	6
KRT2	6
MBD3	5
PPP2R2A	5
KRT9	5
MTA2	5
ZNF687	5
VWA9	4
HSPD1	4
MTA3	4
UBC	3
UBB	3
UBA52	3
RPS27A	3
STUB1	3
TUBA1C	3
TUBA1B	3
PRSS3	3
INTS10	3

SLC25A5	2
TUBB	2
TUBB2B	2
TUBB4B	2
TUBB2A	2
TBB3	2
KRT72	2
ALB	2
KDM1A	2
KDM5D	2
KFM5C	2
NEURL4	2

Mass Spec_4: ZMYND8-SFB FL+IR

Gene symbol	# peptides
ZMYND8	149
CHD4	119
MTA2	46
GATAD2A	43
KDM1A	42
RREB1	38
MTA1	37
PARP1	31
CHD3	29
HSPA8	26
PRKDC	26
HDAC1	24
HSPA5	22
ASUN	21
MBD3	20
HSPA1A	17
RBBP4	17
PHF21A	17
HDAC2	16
ZNF687	16
HIST1H4A	15
HSPA1L	14
HMG20B	14
MTA3	13
INTS10	13
CMAS	11
RCOR1	11
ZNF592	11
RCOR2	11
MBD2	10
VWA9	9
RCOR3	9
HSPA9	9
EMSY	9

KPNA3	8
KPNA2	8
H2AFY	8
SMARCA5	8
RBBP7	7
HSPD1	7
NPM1	7
HIST1H2BB	6
HSPA2	6
RPS7	5
NCL	5
L3MBTL3	5
XRCC5	5
SMARCA4	5
UBA52	4
HIST1H2BA	4
H2AFY2	4
RSF1	4
C7orf26	4
PARP2	4
HNRNPC	4
RBMX	4
SIN3B	4
SFMBT1	4
KDM5A	4
SYNCRIP	4
ACTA2	4
TUBA1A	3
RPS8	3
KPNA4	3
RPL18	3
HIST3H3	3
XRCC6	3
HNRNPH1	3
GATAD1	3
TFAM	3
HNRNPCL1	3
RPS2	3
SMARCC1	3
DDB1	3
SAFB	3
RPS3A	3
HNRNPM	3
SMARCA1	3
PHF20L1	3
HIST1H2AA	2
RPL11	2
RPL7A	2
HIST1H1C	2

EEF1A1	2
HIST1H2BC	2
HIST1H2AD	2
RPS3	2
EMD	2
JMJD1C	2
TMPO	2
HNRNPR	2
H2AFV	2
RPS24	2
PPP2R2A	2
CBX8	2
DNAH7	2
DHX9	2
BAZ1A	2
SAMD1	2
RPL22	2
RPL4	2
SMARCA2	2
TUBB2A	2
RPS18	2
KIF22	2
DNAH9	2
HADHA	2

Supplementary Table 2. Human BRD protein expression vectors used in this study

Gene name	Expression Plasmid	Vector	Gene Source
ASH1L	ASH1L-N-EmGFP	pcDNA6.2/N-EmGFP-DEST	Harvard: HsCD00399413
ATAD2	ATAD2-C-turboGFP	pCMV6-AC-GFP	OriGene: RG218291
BAZ1A (ACF1)	BAZ1A-N-EmGFP	pcDNA6.2/N-EmGFP-DEST	Hela cDNA
	BAZ1A-C-EmGFP	pcDNA6.2/C-EmGFP-DEST	
BAZ1B (WSTF)	BAZ1B-N-EmGFP	pcDNA6.2/N-EmGFP-DEST	U2OS cDNA
	BAZ1B-C-EmGFP	pcDNA6.2/C-EmGFP-DEST	
	BAZ1B-ΔBRD-N-EmGFP	pcDNA6.2/N-EmGFP-DEST	
	BAZ1B-ΔBRD-C-EmGFP	pcDNA6.2/C-EmGFP-DEST	
BAZ2A	BAZ2A-N-EmGFP	pcDNA6.2/N-EmGFP-DEST	DNASU: HsCD00297106
	BAZ2A-C-EmGFP	pcDNA6.2/C-EmGFP-DEST	
BAZ2B	BAZ2B-N-EmGFP	pcDNA6.2/N-EmGFP-DEST	U2OS cDNA
	BAZ2B-C-EmGFP	pcDNA6.2/C-EmGFP-DEST	
BRD1	BRD1-N-EmGFP	pcDNA6.2/N-EmGFP-DEST	DNASU: HsCD00351265
	BRD1-C-EmGFP	pcDNA6.2/C-EmGFP-DEST	
BRD2	BRD2-N-EmGFP	pJTI-R4-Dest-CMV-N-EmGFP	U2OS cDNA
BRD3	BRD3-N-EmGFP	pJTI-R4-Dest-CMV-N-EmGFP	DNASU:HsCD0022366
BRD4	BRD4-N-EmGFP	pcDNA6.2/N-EmGFP-DEST	Addgene:14441
BRD7	BRD7-N-EmGFP	pcDNA6.2/N-EmGFP-DEST	U2OS cDNA
	BRD7-C-EmGFP	pcDNA6.2/C-EmGFP-DEST	
BRD9	BRD9-N-EmGFP	pcDNA6.2/N-EmGFP-DEST	U2OS cDNA
	BRD9-C-EmGFP	pcDNA6.2/C-EmGFP-DEST	
BRDT	BRDT-N-EmGFP	pcDNA6.2/N-EmGFP-DEST	DNASU:HsCD00082651
	BRDT-C-EmGFP	pcDNA6.2/C-EmGFP-DEST	
BRPF1	BRPF1-N-EmGFP	pcDNA6.2/N-EmGFP-DEST	Harvard: HsCD00339323
	BRPF1-C-EmGFP	pcDNA6.2/C-EmGFP-DEST	
BRPF3	BRPF3-N-EmGFP	pcDNA6.2/N-EmGFP-DEST	U2OS cDNA
	BRPF3-C-EmGFP	pcDNA6.2/C-EmGFP-DEST	
BRWD3	BRWD3-N-EmGFP	pcDNA6.2/N-EmGFP-DEST	U2OS cDNA
	BRWD3-C-EmGFP	pcDNA6.2/C-EmGFP-DEST	
CECR2	CECR2-N-EmGFP	pcDNA6.2/N-EmGFP-DEST	DNASU:HsCD00294929
GCN5	GCN5-N-EmGFP	pcDNA6.2/N-EmGFP-DEST	Harvard: HsCD00338147
	GCN5-C-EmGFP	pcDNA6.2/C-EmGFP-DEST	
PBRM1	PBRM1-N-EmGFP	pcDNA6.2/N-EmGFP-DEST	U2OS cDNA
	PBRM1-C-EmGFP	pcDNA6.2/C-EmGFP-DEST	
PCAF	PCAF(Δ5-53a.a.)-N-EmGFP	pcDNA6.2/N-EmGFP-DEST	Harvard: HsCD00343111
	PCAF(Δ5-53a.a.)-C-EmGFP	pcDNA6.2/C-EmGFP-DEST	
PHIP	PHIP-N-EmGFP	pcDNA6.2/N-EmGFP-DEST	Harvard: HsCD00342733
	PHIP-C-EmGFP	pcDNA6.2/C-EmGFP-DEST	
SMARCA2	SMARCA2-N-EmGFP	pcDNA6.2/N-EmGFP-DEST	DNASU:HsCD00082837
	SMARCA2-C-EmGFP	pcDNA6.2/C-EmGFP-DEST	
SMARCA4	SMARCA4-N-EmGFP	pcDNA6.2/N-EmGFP-DEST	Gift from Marcotte lab
	SMARCA4-C-EmGFP	pcDNA6.2/C-EmGFP-DEST	
SP110	SP110A-N-EmGFP	pcDNA6.2/N-EmGFP-DEST	Hela cDNA
	SP110A-C-EmGFP	pcDNA6.2/C-EmGFP-DEST	
	SP110C-N-EmGFP	pcDNA6.2/N-EmGFP-DEST	
	SP110C-C-EmGFP	pcDNA6.2/C-EmGFP-DEST	
SP140	SP140-N-EmGFP	pJTI-R4-Dest-CMV-N-EmGFP	Harvard: HsCD00347023
TAF1	TAF1-N-EmGFP	pcDNA6.2/N-EmGFP-DEST	Harvard: HsCD00399249
	TAF1-C-EmGFP	pcDNA6.2/C-EmGFP-DEST	
TRIM24	TRIM24-N-EmGFP	pcDNA6.2/N-EmGFP-DEST	DNASU:HsCD00005267

	TRIM24-C-EmGFP	pcDNA6.2/C-EmGFP-DEST	
TRIM28 (KAP1)	TRIM28-N-EmGFP	pcDNA6.2/N-EmGFP-DEST	U2OS cDNA
	TRIM28-C-EmGFP	pcDNA6.2/C-EmGFP-DEST	
	TRIM28-ΔBRD-N-EmGFP	pcDNA6.2/N-EmGFP-DEST	
	TRIM28-ΔBRD-C-EmGFP	pcDNA6.2/C-EmGFP-DEST	
TRIM33	TRIM33-N-EmGFP	pcDNA6.2/N-EmGFP-DEST	Addgene:15734
	TRIM33-C-EmGFP	pcDNA6.2/C-EmGFP-DEST	
TRIM66	TRIM66-N-EmGFP	pcDNA6.2/N-EmGFP-DEST	HT1080 cDNA
	TRIM66-C-EmGFP	pcDNA6.2/C-EmGFP-DEST	
ZMYND8	ZMYND8-N-EmGFP	pcDNA6.2/N-EmGFP-DEST	U2OS cDNA
	ZMYND8-C-EmGFP	pcDNA6.2/C-EmGFP-DEST	
	ZMYND8 N248A-N-EmGFP	pcDNA6.2/N-EmGFP-DEST	
	ZMYND8-ΔBRD-N-EmGFP	pcDNA6.2/N-EmGFP-DEST	
	ZMYND8-SFB	GW-C-SFB-DEST	
	ZMYND8-ΔPBP-SFB	GW-C-SFB-DEST	
	ZMYND8-ΔC-1-SFB	GW-C-SFB-DEST	
	ZMYND8-ΔC-2-SFB	GW-C-SFB-DEST	
	ZMYND8-ΔC-3-SFB	GW-C-SFB-DEST	
	ZMYND8-ΔMYND-SFB	GW-C-SFB-DEST	
	ZMYND8-ΔInter-SFB	GW-C-SFB-DEST	
	GST-PB-His	DEST15	
ZMYND11	ZMYND11-N-EmGFP	pcDNA6.2/N-EmGFP-DEST	U2OS cDNA
	ZMYND11-C-EmGFP	pcDNA6.2/C-EmGFP-DEST	

Supplementary Table 3. Antibody list.

Antibody epitope	Mono/polyclonal	Host	Source	Catalog No.	Application
ATAD2B	Polyclonal	Rabbit	Abnova	PAB22621	IF
Actetyl-Histone H3 (lys 9)	Polyclonal	Rabbit	Millipore	06-942	WB
Actetyl-Histone H3 (lys 27)	Polyclonal	Rabbit	Millipore	07-360	WB
Actetyl-Histone H3 (lys 56)	Monoclonal	Rabbit	Epitomics	2134	WB
Actetyl-Histone H4 (lys16)	Polyclonal	Rabbit	Cell Signaling	8804	WB
Actetyl-Histone H4 (lys 5, 8, 12 and 16)	Polyclonal	Rabbit	Millipore	06-866	WB
BRD8	Polyclonal	Rabbit	Abcam	ab17969	IF
BRWD1	Polyclonal	Mouse	Abnova	H00054014	IF
BPTF	Polyclonal	Rabbit	Bethyl	A300-973A	IF
CBP	Monoclonal	Rabbit	Cell Signaling	7389	IF
CHD4	Polyclonal	Rabbit	Active Motif	39289	IF, IP, WB
CHK1	Monoclonal	Mouse	Santa Cruz	sc-8408	WB
CHK2	Polyclonal	Rabbit	Cell Signaling	2662	WB
CtIP	Monoclonal	Rabbit	Cell Signaling	9201	WB
DNA-PKcs	Monoclonal	mouse	Abcam	ab1832	WB
DNA-PKcs S2056p	Polyclonal	Rabbit	Abcam	ab18192	WB
Flag	Monoclonal	Mouse	Sigma	F1804	WB
GFP	Polyclonal	Rabbit	Invitrogen	A11122	IP, WB
GST	Polyclonal	Goat	GE Healthcare	27-4577	WB
H2AX	Polyclonal	Rabbit	Cell Signaling	2595	WB
H3	Polyclonal	Rabbit	Abcam	ab1791	WB
H4	Polyclonal	Rabbit	Abcam	ab124762	WB
HDAC1	Polyclonal	Rabbit	Abcam	ab19845	WB
HDAC2	Polyclonal	Rabbit	Abcam	ab7029	WB
LSD1	Polyclonal	Rabbit	Active Motif	39186	IF, WB
MLL	Polyclonal	Rabbit	Millipore	ABE240	IF
p300	Monoclonal	Mouse	Millipore	05-257	IF
p53	Monoclonal	Mouse	Active Motif	39553	WB
Phospho-CHK1 (Ser345)	Monoclonal	Rabbit	Cell Signaling	2348	WB
Phospho-CHK2 (Thr68)	Polyclonal	Rabbit	Cell Signaling	2661	WB
Phospho-p53 (Ser15)	Polyclonal	Rabbit	Cell Signaling	9284	WB
RAD51	Polyclonal	Rabbit	Santa Cruz	sc-8349	ChIP
RAD51	Polyclonal	Mouse	Abcam	ab88572	IF
SP100	Polyclonal	Rabbit	Enzo	BML-PW0325	IF
XRCC4	Polyclonal	Rabbit	Abcam	ab145	ChIP
ZMYND8	Polyclonal	Rabbit	Sigma	HPA020949	WB
ZMYND8	Polyclonal	Rabbit	Bethyl	A302-089A	IP, WB
β-tubulin	Polyclonal	Rabbit	Abcam	ab6046	WB
γH2AX	Polyclonal	Rabbit	Novus	NB100-384	IF, WB
γH2AX	Monoclonal	Mouse	Millipore	05-636	IF

ChIP: chromatin immunoprecipitation; IF: immunofluorescence; IP: immunoprecipitation; WB: Western blotting